Environmental controls on seasonal ecosystem evapotranspiration/potential evapotranspiration ratio as determined by the global eddy flux measurements

Chunwei Liu[1], Ge Sun[2*], Steve G. McNulty[2], Asko Noormets[3], and Yuan Fang[3]

1. Jiangsu Provincial Key Laboratory of Agricultural Meteorology, College of Applied Meteorology, Nanjing University of Information Science and Technology, Nanjing 210044, China;
2. Eastern Forest Environmental Threat Assessment Center, Southern Research Station, USDA Forest Service, Raleigh, NC 27606, USA;
3. Department of Forestry and Environmental Resources, North Carolina State University, Raleigh, NC 27695, USA.

**Corresponding author:* Ge Sun, 920 Main Campus Dr., Venture II, Suite 300, Raleigh, NC 27606, USA. gesun@fs.fed.us; (919)5159498 (Phone); (919)5132978(Fax)

Abstract: The evapotranspiration/potential evapotranspiration **(**AET/PET) ratio is traditionally termed as crop coefficient (*Kc*) and has been ~~gradually~~ used as ecosystem evaporative stress index. In the current hydrology literature, *Kc* has been widely used to as a parameter to estimate crop water demand by water managers, but has not been well examined for other type of ecosystems such as forests and other perennial vegetation. Understanding the seasonal dynamics of this variable for all ecosystems is important to project the ecohydrologcial responses to climate change and accurately quantify water use (AET) at watershed to global scales. This study aimed at deriving monthly *Kc* for multiple vegetation cover types and understanding its environmental controls by analyzing the accumulated global eddy flux (FLUXNET) data. We examined monthly AET/PET data for 7 vegetation covers including Open shrubland (OS), Cropland (CRO), Grassland (GRA), Deciduous broad leaf forest (DBF), Evergreen needle leaf forest (ENF) and Evergreen broad leaf forest (EBF), and Mixed forest (MF) across 81 sites. We found that, except for evergreen forests (EBF and ENF), *Kc* values had large seasonal variation across all land covers. The spatial variability of *Kc* was best explained by latitude suggesting site factors ~~has~~ a major control on *Kc*. Seasonally, *Kc* increased significantly with precipitation in the summer months. Moreover, Leaf Area Index (LAI) significantly influenced monthly *Kc* in all land covers except EBF. During the peak growing season, forests had the highest *Kc* values while Croplands (CRO) had the lowest. We developed a series of multi-variate linear monthly regression models for a large spatial scale *Kc* by land cover type and season using LAI, site latitude and monthly precipitation as independent variables. The *Kc* models are useful for understanding water stress in different ecosystems under climate change and variability ~~and~~ for estimating seasonal ET for large areas with mixed land covers.

Key words: crop coefficient, evapotranspiration, eddy covariance, modeling, water stress

1. Introduction

Evapotranspiration (ET) is one of the major hydrological processes that link energy, water, and carbon cycles in terrestrial ecosystems (Fang et al., 2015;Sun et al., 2010; Sun et al., 2011a; Sun et al., 2011b). In contrast to potential ET (PET) that depends only on atmospheric water demand (Lu et al., 2005), actual evapotranspiration (AET) is arguably the most uncertain ecohydrologic variable for quantifying watershed water budgets (Baldocchi and Ryu, 2011;Fang et al., 2015;Hao et al., 2015a) and for understanding the ecological impacts of climate and land use change (Hao et al., 2015b), and climate variability (Hao et al., 2014). In recent years, one of the most important research questions of ecohydrology focused on how ecosystem dynamics, precipitation, AET, and PET interact in different ecosystems at seasonal and long term scales under a changing environment (Vose et al., 2011).

The ratio of AET to PET is traditionally termed as crop coefficient (*Kc*), and has been widely used to as a parameter to estimate crop water demand by water managers (Allen and Pereira, 2009;Irmak et al., 2013a).However, this parameter has not been well examined for other ecosystems(Zhou et al., 2010;Zhang et al., 2012). The ratio of AET to PET has also been used as an indicator of regional terrestrial water availability, wetness or drought index, and plant water stress (Anderson et al., 2012;Mu et al., 2012).When the annual AET/PET ratio is close to 1.0, the soil water meets ecosystem water use demand. The ratio of AET/PET or water stress level can be drastically different among different ecosystems in different environmental conditions, because AET is mainly controlled by climate (precipitation and PET) (Zhang et al., 2001) and ecosystem species composition and

structure (i.e., leaf area index, rooting depth) (Sun et al., 2011a). The seasonal PET values for a particular region are generally stable (Rao et al., 2011;Lu et al., 2005), and deviation of AET/PET from the norm indicates variability in AET, which responds to precipitation and water availability when PET is stable (Rao et al., 2011). However, under a changing climate, the monthly AET/PET patterns can be rather complex since both AET and PET are affected by air temperature and precipitation (Sun et al., 2015b;Sun et al., 2015a) and corresponding changes in ecosystem characteristics (e.g., plant species shift) (Sun et al., 2014;Vose et al., 2011).

In the agricultural water management community, the crop coefficient method remains a popular one for approximating crop water use, despite recent advances in direct ET measurement methods (Baldocchi et al., 2001;Fang et al., 2015;Allen et al., 1998;Allen and Pereira, 2009). The *Kc* is termed as single crop coefficient (Allen et al., 1998;Allen et al., 2006;Tabari et al., 2013) which is affected by growing periods, crop species, canopy conductance, and soil evaporation in the field scale (Ding et al., 2015;Allen et al., 1998;Shukla et al., 2014b). Moreover, *Kc* can be influenced by soil characteristics, vegetative soil cover, height, plant species distribution, and leaf area index in a larger spatial scale (Descheemaeker et al., 2011;Consoli and Vanella, 2014;Anda et al., 2014). Although the Food and Agriculture Organization of the United Nations provides various guidelines for several crops (Allen et al., 1998), local measurements are still required to estimate *Kc* to account for local crop varieties and for year-to-year variation in weather conditions (Pereira et al., 2015).

Although the *Kc* method has been widely used for estimating AET for crops, it has not been widely used for natural ecosystems for the purpose of estimating AET due to limited

continuous measurements in these systems. However, as discussed earlier, ecologists and hydrologist have started to use *Kc* to quantify ecosystem stress levels, and consider *Kc* as a variable rather than a constant. Past studies found that *Kc* was influenced by the growing stages and leaf area index for maize (Kang et al., 2003;Ding et al., 2015), winter wheat(Kang et al., 2003;Allen et al., 1998), watermelon (Shukla et al., 2014b), and fruit trees (Marsal et al., 2014b;Taylor et al., 2015). Variations of mid-season crop coefficients for a mixed riparian vegetation dominated by common reed (*Phragmites australis*) could be predicted by growing degree days in central Nebraska, USA(Irmak et al., 2013a). *Kc* ranged from 0.50 to 0.85 for small, open grown shrubs, and from 0.85 to 0.95 for well-developed shrubland. The *Kc* values had a close logarithmic relationship with the canopy cover fraction in the highlands of northern Ethiopia (Descheemaeker et al., 2011). Overall, the non-agricultural ecosystems such as forests, grasslands and shrublands are heterogeneous in nature and have high soil water availability. Thus, *Kc* values for natural ecosystems have high variability (Allen et al., 2011;Allen and Pereira, 2009).

Therefore, the goal of this study was to explore how *Kc* varies among multiple ecosystems with various vegetation types over multiple seasons. Another goal was to determine the key biophysical and environmental factors such as latitude, precipitation, and leaf area index that could be used to estimate *Kc*, and if *Kc* can be modeled with a reasonable accuracy in a larger spatial scale. We examined the *Kc* variations for seven land cover types by analyzing the FLUXNET eddy flux data (Baldocchi et al., 2001;Fang et al., 2015). Specifically, our objectives were to 1) understand the variation of monthly *Kc* for seven distinct land covers by analyzing the influences of environmental factors (e.g., precipitation, site latitude) on *Kc*; and 2) to develop simple land-cover specific regression

models for estimating *Kc* with key environmental factors as independent variables. Specifically, we developed quantitative relationships between environmental factors and *Kc* by land cover type using data from FLUXNET sites for 8 croplands(CRO), 13 deciduous broad leaf forests(DBF), 2 evergreen broad leaf forests(EBF), 34 evergreen needle leaf forests (ENF), 9 grasslands (GRA), 10 mixed forests (MF), and 2 open shrublands (OS). In-depth understanding of the biophysical controls on *Kc* for different ecosystems is important for accurately estimating AET and anticipating the impacts of climate change on ecosystem water stress and water balances.

2. Methods

This synthesis study used the LaThuile eddy flux dataset that was developed by FLUXNET (http://fluxnet.ornl.gov/; Fig. 1), a global network that measures the exchanges of carbon dioxide, water vapor, and energy between the biosphere and atmosphere (Baldocchi et al., 2001). The FLUXNET data (Baldocchi et al., 2001;Baldocchi and Ryu, 2011) have been widely used to understand the evapotranspiration processes and trend (Fang et al., 2015;Jung et al., 2010), develop AET and ecosystem models (Sun et al., 2011b;Zhang et al., 2016) and map continental-scale ecosystem productivity (Xiao et al., 2014;Zhang et al., 2016).

We used an existing database that was developed from the eddy flux measurements from 108 sites (Fang et al., 2015). A total of 78 sites were selected to calculate monthly *Kc* for multiple years and develop *Kc* models for different ecosystems, and 30 sites were used for validating the models. According to the International Geosphere-Biosphere

Program (IGBP) land cover classification system, these eddy flux sites represent nine land cover types: open shrubland (OS), cropland (CRO), grassland (GRA), deciduous broad leaf forest (DBF), evergreen needle leaf forest (ENF) and evergreen broad leaf forest (EBF), and mixed forest (MF). For each eddy flux tower site (Figure 1), we acquired AET and associated micro-meteorological data, such as vapor pressure deficit, precipitation (P), winds speed, net radiation. Potential daily evapotranspiration (PET) was calculated by the FAO Penman–Monteith equation as follows (Allen et al., 1998):

$$\mathrm{PET} = \frac{0.408\Delta\left(R_n - G\right) + \gamma \frac{900}{T+273} u_2 \left(e_s - e_a\right)}{\Delta + \gamma\left(1 + 0.34u_2\right)} \quad (1)$$

where R_n is net radiation at the cover surface (MJ m^{-2} d^{-1}), G is soil heat flux (MJ m^{-2} d^{-1}), T is mean air temperature (°C), u_2 is wind speed (m s^{-1}), e_s is saturation vapour pressure (kP_a), e_a is actual vapour pressure (kP_a), e_s–e_a is the saturation vapour pressure deficit (kP_a), Δ is slope of saturation vapour pressure curve (kP_a °C^{-1}), and γ is the psychrometric constant (kP_a °C^{-1}).

The monthly crop coefficient (*Kc*) is defined as the ratio of the measured total monthly AET and the total monthly PET calculated by Equation 1 varies by month and vegetation types (Equation 2). The average annual *Kc* were calculated using mean monthly *Kc* from January to December for the special sites.

$$Kc = \frac{ET}{ET_0} \quad (2)$$

The LAI time series for each tower site were downloaded from the Oak Ridge National Laboratory Distributed Active Archive Center (http://daac.ornl.gov/cgi-bin/MODIS/GR_col5_1/mod_viz.html). MODIS LAI was derived from the fraction of

absorbed photosynthetically active radiation (FPAR) that a plant canopy absorbs for photosynthesis and growth in the 0.4–0.7 nm spectral range. The MODIS LAI/FPAR algorithm exploits the spectral information of MODIS surface reflectance at up to seven spectral bands. We extracted monthly LAI data for the time period from 2000 through 2006 across 77 sites using 8-day GeoTIFF data from the Moderate Resolution Imaging Spectroradiometer (MODIS) land subsets' 1-km LAI global fields. We estimated monthly LAI for each flux tower by computing the mean of the 8-day daily values for each month (Fang et al., 2015).

3. Results

3.1. Seasonal variations and long term means of Kc by land cover

The average monthly *Kc* based on eddy flux data from 2000 to 2007 increased gradually from January to July and then decreased (Fig. 2). EBF had the highest mean monthly *Kc* (1.01±0.17) (mean ± standard error) in August. *Kc* for both EBF and ENF varied less seasonally than other forest types (Fig. 2). Standard errors for GRA, ENF and OS (0.10-0.17) were larger than other land cover types (0.03-0.10) for April to August. EBF had higher *Kc* for all seasons than other land covers with a peak value of 0.91 (± 0.13) in the summer season (Fig. 3). In winter seasons, CRO and OS had the lowest *Kc*, 0.25 (± 0.006) and 0.22 (± 0.004), respectively.

The mean annual *Kc* was 0.39 (± 0.04), 0.47 (± 0.05), 0.79 (± 0.03), 0.45 (± 0.02), 0.57 (± 0.06), 0.45 (± 0.05), and 0.40 (± 0.04) for CRO, DBF, EBF, ENF, GRA, MF, and OS, respectively. Yearly average precipitation was higher in EBF and DBF than other land covers (Fig. 4). The precipitation ranking by land cover type was DBF> EBF> MF>

GRA> ENF> CRO> OS. Consequently, OS, MF, GRA and ENF had relatively low AET (376-425 mm). In contrast, CRO had relatively low precipitation with a high PET.

3.2. Environmental controls on Kc

As indicated in Equation 1, factors such as temperature and solar radiation were ~~using~~ for PET calculation, and were not independent to AET/PET. Therefore, we chose other independent factors to simulate AET/PET. ~~Since site~~ latitude is a readily available variable for a particular location, but is crucial to ~~determine~~ the day length and incoming radiation over the year in the same land cover types, so we explored the relationship between *Kc* and site latitude.

The results show that annual *Kc* was negatively (p<0.05) correlated with the latitude of the sites (Fig.5) for CRO, DBF, ENF, GRA and MF with a determination coefficient (R^2) of 0.83, 0.59 and 0.21, 0.72 and 0.52, respectively. For OS, annual mean *Kc* also decreased with the increase in site latitude. Most of the study site latitudes fell between 30 °N to 60 °N.

At the seasonal scale, the linear relationships between monthly *Kc* and total monthly precipitation differed among different land cover types (Fig. 6). Monthly *Kc* increased with monthly precipitation in the same ecosystem type with the R^2 ranking from high to low: OS>MF>GRA>ENF>CRO>DBF. The monthly *Kc* for open shrublands (OS) was especially sensitive to precipitation (R^2= 0.69, p<0.001). The monthly *Kc* for EBF was not as sensitive to precipitation because EBF was generally found in a wet environment with a peak monthly precipitation of 468 mm. Moreover, *Kc* for OS, GRA and MF in relatively drier environments had lower values (Fig. 2). Therefore, *Kc* was closely related to the monthly precipitation.

In addition to growing season, site latitude and monthly precipitation, leaf area index affected the monthly *Kc* (Fig. 7). *Kc* was obviously influenced by the leaf area index (LAI) for all land covers. The determination coefficients for different land covers were OS> MF=GRA> ENF>DBF>CRO>EBF. The LAI range was up to 6 m^2 m^{-2} in most land covers, while it only reached 3-4 m^2 m^{-2} in OS and CRO.

3.3. Kc models

A series empirical *Kc* model ~~was~~ developed using a multiple linear regression approach with precipitation, leaf area index (LAI), and site latitude as independent variables (Table 1).The monthly precipitation, LAI and site latitude influenced *Kc* (p<0.1) for most ecosystems studied in different seasons except at EBF in spring, fall and winter, and for OS in the spring. As annual precipitation increases, total leaf area increases, therefore *Kc* increases for ENF in all seasons and most of the time for DBF and MF. As site latitude increases, *Kc* values were found to decrease in some periods at CRO, DBF and MF sites. In addition, *Kc* was closely correlated to LAI, site latitude, and monthly precipitation at ENF in fall and OS in winter with R^2 0.55 and 0.99. All land covers had ~~a~~ peak values (0.53 $\pm$ 0.04- 1.01 $\pm$ 0.17) in the summer months. Except for EBF and GRA, *Kc* values had a close relationship with the monthly precipitation in the summer with R^2 ranging from 0.21 to 0.90. The linear relationships were significant for most vegetation types, suggesting the regression models (Table 1) can be used to estimate monthly *Kc* if LAI and precipitation for a specific ecosystem are available.

3.4. The validation of the regression models of Kc

All *Kc* multiple regression models for different seasons were validated ~~by~~ecosystem type (Fig. 8). The validation was carried out for 30 sites at a monthly scale. The results showed that the modeled AET calculated from the multiple *Kc* models compared well with measurmentswith R^2 ranging 0.28-0.56. Among the ecosystems, the model for DBF appeared to be the most accurate one with a R^2 of 0.56.

4. Discussion

Our study estimated annual and seasonal crop coefficient (*Kc*) for seven land cover types using measured global eddy flux data. We comprehensively evaluated environmental controls (i.e., precipitation, LAI, and site latitude) on annual and growing seasons ~~s~~ *Kc* and developed a series of multiple linear regression models that can be used for estimating monthly AET over time and space.

4.1. Crop coefficient variation in different seasons

Several recent studies had shown that *Kc* reached the maximum value in middle of the growing season in many ecosystems, such as a *P. euphratica* forest in the riparian area (Hou et al., 2010)in a desert environment, a watermelon crop covered with plastic mulch in Florida (Shukla et al., 2014b;Shukla et al., 2014a), soybean in Nebraska (Irmak et al., 2013b), a temperate desert steppe in Inner Mongolia(Zhang et al., 2012). As Fig. 2 shows, most of the land covers had peak *Kc* during June to August, while the seasonal patterns of ENF and EBF varied less than other surfaces. Vegetation growth for both the ENF and EBF sites is active throughout the year. The crop coefficients for early period mid-density fruit trees is about 0.5 (Allen et al., 1998;Allen and Pereira, 2009) which is similar to those found for DBF or MF during April and May. In addition, the middle season *Kc* values for apple and peach trees with active ground cover were higher than *Kc* for DBF sites during

the summer. It is likely that the orchards had higher evapotranspiration rates than natural forests due to irrigation in orchards.

4.2. Environmental control factors for Kc

The ecosystem covers and the distributions of the vegetation classes were determined by the latitude (Potter et al., 1993). Crop coefficient varies predominately by ecosystems, *Kc* will in most cases increase as the site latitude decreased for the same land cover (Fig. 5). As the latitude decreased, the temperature and the solar radiation increased and the vegetation characteristics would be different for the same land cover type. Models developed from the FLUXNET data may be best used on flat areas for a given latitude given that eddy covariance towers were generally installed on flat lands (Baldocchi et al., 2001). For areas with complex topography, the relationship between *Kc* and site latitude may be more complicated.

Spatial variations of *Kc* are characteristic of ecosystems, but *Kc* is also affected by climate factors such as rainfall. For example, *Kc* was highly correlated with precipitation for most land covers (Fig. 6).The rainfall is the major source of soil water and AET in natural ecosystems (Parent and Anctil, 2012). During dry years or periods, a lack of precipitation may cause a reduction of the leaf area index and *Kc* will decrease ~~to response the ecosystem function~~. During rainy seasons, as, leaf area index and stomatal conductance of trees and rain-fed crops increases, so does *Kc* (Kar et al., 2006;Zeppel et al., 2008). Irrigation of cropland is a primary mechanism for increasing yield (Du et al., 2015;Fereres and Soriano, 2007), so the CRO may have a high monthly *Kc* even at sites with a low precipitation. In contrast, *Kc* does not have a close relationship with precipitation under a

wet environment. For example, the EBF site had a monthly precipitation as high as 468 mm/month and generally exceeded monthly AET. In an opposite case for the OS sites, monthly precipitation values were between 0.7 to 69 mm, and *Kc* was highly correlated to monthly precipitation. Moreover, the soil moisture could be a limiting factor to AET, and would affect *Kc* in dry periods. ~~When the~~ time lag between precipitation and soil moisture might cause errors in modeling *Kc* in the long dry or wet season. However, at the monthly scale, previous modeling work (Fang et al., 2015) suggest that considering a time lag does not increase the prediction power dramatically (G. Sun Personal communication).

Besides precipitation, leaf area index (LAI) also affects *Kc* in dry and semi-humid area (Zhang et al., 2012;Kang et al., 2003). Unlike precipitation, LAI directly affects *Kc* in AET calculations (Nov ák, 2012;Tolk and Howell, 2001). Inter-annual *Kc* values are stable at the GRA and OS sites due to the steady seasonal LAI between years while the plantation forest sites had a more dynamic LAI pattern(Marsal et al., 2014a). As the growth rate of the perennial plants could have large effects on relationship between *Kc* and LAI, long term data are needed to estimate *Kc* as a function of all environmental factors.

4.3. Modeling the dynamics of Kc

Our study results are consistent with previous studies that show that the growing stage is a key factor for estimating *Kc* in agricultural crops (Allen et al., 1998;Zhang et al., 2013;Wei et al., 2015;Alberto et al., 2014), fruit trees (Abrisqueta et al., 2013;Marsal et al., 2014b), salt grass (Bawazir et al., 2014) and *Populus euphratica Oliv* forest (Hou et al., 2010). Additionally, our study showed that *Kc* fluctuated more dramatically in DBF, GRA, and MF than other land covers in different seasons (Table 1). Studies also show that monthly

leaf resistance that varies over time is important in estimating the seasonal crop coefficient for a citrus orchard (Taylor et al., 2015). The LAI and total monthly precipitation were considered as independent factors (Bond-Lamberty and Thomson, 2010) and both of them varied in both time and space while the site latitude only represents spatial influences on *Kc*. The modeled AET was acceptable for the different land cover types (Fig. 8), and could be used for monthly AET calculation for large spatial scale and homogeneous ecosystems. Thus, the multiple linear regression equations developed from this study take account of both spatial and temporal changes in land surface characteristics and offer a powerful tool to estimate ~~of~~ seasonal ~~dynamic~~ *Kc* for different ecosystems (Table 1).

5. Conclusions

To seek a convenient method to calculate monthly AET ~~in~~ large spatial scale, we comprehensively examined the relations between *Kc* and environmental factors using eddy flux data from 81 sites with different land covers. We found that *Kc* values varied largely among CRO, DBF, EBF, GRA and MF and over seasons. Precipitation determined *Kc* in the growing seasons (such as summer), and was chosen as a key variable to calculate *Kc*. We established multiple linear equations for different land covers and seasons to model the dynamics of *Kc* as function of LAI, site latitude and monthly precipitation. These empirical models could be helpful in calculating monthly AET at the regional scale~~s~~ with readily available climatic data and vegetation structure information. Our study extended the applications of the traditional *Kc* method for estimating crop water use to estimating AET rates and evaporative stress for natural ecosystems. Future studies should further test the applicability of the empirical *Kc* models under extreme climatic conditions.

References

Abrisqueta, I., Abrisqueta, J. M., Tapia, L. M., Mungu á, J. P., Conejero, W., Vera, J., and Ruiz-S ánchez, M. C.: Basal crop coefficients for early-season peach trees, Agricultural Water Management, 121, 158-163, http://dx.doi.org/10.1016/j.agwat.2013.02.001, 2013.

Alberto, M. C. R., Quilty, J. R., Buresh, R. J., Wassmann, R., Haidar, S., Correa, T. Q., and Sandro, J. M.: Actual evapotranspiration and dual crop coefficients for dry-seeded rice and hybrid maize grown with overhead sprinkler irrigation, Agricultural Water Management, 136, 1-12, 10.1016/j.agwat.2014.01.005, 2014.

Allen, R. G., Pereira, L. S., Raes, D., and Smith, M.: Crop evapotranspiration, FAO irrigation and drainage paper No. 56, 1998.

Allen, R. G., Pruitt, W. O., Wright, J. L., Howell, T. A., Ventura, F., Snyder, R., Itenfisu, D., Steduto, P., Berengena, J., Yrisarry, J. B., Smith, M., Pereira, L. S., Raes, D., Perrier, A., Alves, I., Walter, I., and Elliott, R.: A recommendation on standardized surface resistance for hourly calculation of reference ETo by the FAO56 Penman-Monteith method, Agricultural Water Management, 81, 1-22, http://dx.doi.org/10.1016/j.agwat.2005.03.007, 2006.

Allen, R. G., and Pereira, L. S.: Estimating crop coefficients from fraction of ground cover and height, Irrigation Science, 28, 17-34, DOI 10.1007/s00271-009-0182-z, 2009.

Allen, R. G., Pereira, L. S., Howell, T. A., and Jensen, M. E.: Evapotranspiration information reporting: I. Factors governing measurement accuracy, Agricultural Water Management, 98, 899-920, http://dx.doi.org/10.1016/j.agwat.2010.12.015, 2011.

Anda, A., Silva, J. A. T. d., and Soos, G.: Evapotranspiration and crop coefficient of common reed at the surroundings of Lake Balaton, Hungary, Aquatic Botany, 116, 53-59, 10.1016/j.aquabot.2014.01.008, 2014.

Anderson, M. C., Allen, R. G., Morse, A., and Kustas, W. P.: Use of Landsat thermal imagery in monitoring evapotranspiration and managing water resources, Remote Sensing of Environment, 122, 50-65, 2012.

Baldocchi, D., Falge, E., Gu, L., Olson, R., Hollinger, D., Running, S., Anthoni, P., Bernhofer, C., Davis, K., and Evans, R.: FLUXNET: A new tool to study the temporal and spatial variability of ecosystem-scale carbon dioxide, water vapor, and energy flux densities, Bulletin of the American Meteorological Society, 82, 2415-2434, 2001.

Baldocchi, D. D., and Ryu, Y.: A synthesis of forest evaporation fluxes–from days to years–as measured with eddy covariance, in: Forest Hydrology and Biogeochemistry, Springer, 101-116, 2011.

Bawazir, A. S., Luthy, R., King, J. P., Tanzy, B. F., and Solis, J.: Assessment of the crop coefficient for saltgrass under native riparian field conditions in the desert southwest, Hydrological Processes, 28, 6163-6171, Doi 10.1002/Hyp.10100, 2014.

Bond-Lamberty, B., and Thomson, A.: Temperature-associated increases in the global soil respiration record, Nature, 464, 579-582, 2010.

Consoli, S., and Vanella, D.: Mapping crop evapotranspiration by integrating vegetation indices into a soil water balance model, Agricultural Water Management, 143, 71-81, 10.1016/j.agwat.2014.06.012, 2014.

Descheemaeker, K., Raes, D., Allen, R., Nyssen, J., Poesen, J., Muys, B., Haile, M., and Deckers, J.: Two rapid appraisals of FAO-56 crop coefficients for semiarid natural vegetation of the northern Ethiopian highlands, Journal Of Arid Environments, 75, 353-359, DOI 10.1016/j.jaridenv.2010.12.002, 2011.

Ding, R. S., Tong, L., Li, F. S., Zhang, Y. Q., Hao, X. M., and Kang, S. Z.: Variations of crop coefficient and its influencing factors in an arid advective cropland of northwest China, Hydrological Processes, 29, 239-249, Doi 10.1002/Hyp.10146, 2015.

Du, T., Kang, S., Zhang, J., and Davies, W. J.: Deficit irrigation and sustainable water-resource strategies in agriculture for China's food security, J Exp Bot, 66, 2253-2269, 10.1093/jxb/erv034, 2015.

Fang, Y., Sun, G., Caldwell, P., McNulty, S. G., Noormets, A., Domec, J. C., King, J., Zhang, Z., Zhang, X., and Lin, G.: Monthly land cover - specific evapotranspiration models derived from global eddy flux measurements and remote sensing data, Ecohydrology, 2015.

Fereres, E., and Soriano, M. A.: Deficit irrigation for reducing agricultural water use, Journal of experimental botany, 58, 147-159, 2007.

Hao, L., Sun, G., Liu, Y., Gao, Z., He, J., Shi, T., and Wu, B.: Effects of precipitation on grassland ecosystem restoration under grazing exclusion in Inner Mongolia, China, Landscape Ecology, 1-17, 10.1007/s10980-014-0092-1, 2014.

Hao, L., Sun, G., Liu, Y., and Qian, H.: Integrated Modeling of Water Supply and Demand under Management Options and Climate Change Scenarios in Chifeng City, China, JAWRA Journal of the American Water Resources Association, 51, 655-671, 2015a.

Hao, L., Sun, G., Liu, Y., Wan, J., Qin, M., Qian, H., Liu, C., Zheng, J., John, R., and Fan, P.: Urbanization dramatically altered the water balances of a paddy field-dominated basin in southern China, Hydrology and Earth System Sciences, 19, 3319-3331, 2015b.

Hou, L. G., Xiao, H. L., Si, J. H., Xiao, S. C., Zhou, M. X., and Yang, Y. G.: Evapotranspiration and crop coefficient of Populus euphratica Oliv forest during the growing season in the extreme arid region northwest China, Agricultural Water Management, 97, 351-356, 2010.

Irmak, S., Kabenge, I., Rudnick, D., Knezevic, S., Woodward, D., and Moravek, M.: Evapotranspiration crop coefficients for mixed riparian plant community and transpiration crop coefficients for Common reed, Cottonwood and Peach-leaf willow in the Platte River Basin, Nebraska-USA, Journal of Hydrology, 481, 177-190, 10.1016/j.jhydrol.2012.12.032, 2013a.

Irmak, S., Odhiambo, L. O., Specht, J. E., and Djaman, K.: Hourly And Daily Single And Basal Evapotranspiration Crop Coefficients as a Function Of Growing Degree Days, Days after Emergence, Leaf Area Index, Fractional Green Canopy Cover, And Plant Phenology for Soybean, T Asabe, 56, 1785-1803, 2013b.

Jung, M., Reichstein, M., Ciais, P., Seneviratne, S. I., Sheffield, J., Goulden, M. L., Bonan, G., Cescatti, A., Chen, J., and De Jeu, R.: Recent decline in the global land evapotranspiration trend due to limited moisture supply, Nature, 467, 951-954, 2010.

Kang, S., Gu, B., Du, T., and Zhang, J.: Crop coefficient and ratio of transpiration to evapotranspiration of winter wheat and maize in a semi-humid region, Agricultural water management, 59, 239-254, 2003.

Kar, G., Verma, H. N., and Singh, R.: Effects of winter crop and supplemental irrigation on crop yield, water use efficiency and profitability in rainfed rice based cropping system of eastern India, Agricultural Water Management, 79, 280-292, DOI 10.1016/j.agwat.2005.03.001, 2006.

Lu, J., Sun, G., McNulty, S. G., and Amatya, D.: A comparison of six potential evapotranspiration methods for regional use in the Southeastern United States, 2005.

Marsal, J., Casadesus, J., Lopez, G., Girona, J., and Stöckle, C.: Disagreement between tree size and crop coefficient in'conference'pear: comparing measurements by a weighing Lysimeter and prediction by Cropsyst, Acta horticulturae, 2014a.

Marsal, J., Johnson, S., Casadesus, J., Lopez, G., Girona, J., and Stöckle, C.: Fraction of canopy intercepted radiation relates differently with crop coefficient depending on the season and the fruit tree species, Agricultural and Forest Meteorology, 184, 1-11, http://dx.doi.org/10.1016/j.agrformet.2013.08.008, 2014b.

Mu, Q., Zhao, M., Kimball, J., McDowell, N., and Running, S.: A remotely sensed global terrestrial drought severity index, in: Evapotranspiration in the Soil-plant-atmosphere System, AGU Fall Meeting Abstracts, 2012, L02, 2012.

Novák, V.: Evapotranspiration in the Soil-plant-atmosphere System, Springer Science & Business Media, 2012.

Parent, A. C., and Anctil, F.: Quantifying evapotranspiration of a rainfed potato crop in South-eastern Canada using eddy covariance techniques, Agricultural Water Management, 113, 45-56, DOI 10.1016/j.agwat.2012.06.014, 2012.

Pereira, L. S., Allen, R. G., Smith, M., and Raes, D.: Crop evapotranspiration estimation with FAO56: Past and future, Agricultural Water Management, 147, 4-20, 2015.

Potter, C. S., Randerson, J. T., Field, C. B., Matson, P. A., Vitousek, P. M., Mooney, H. A., and Klooster, S. A.: Terrestrial ecosystem production: a process model based on global satellite and surface data, Global Biogeochemical Cycles, 7, 811-841, 1993.

Rao, L., Sun, G., Ford, C., and Vose, J.: Modeling potential evapotranspiration of two forested watersheds in the southern Appalachians, Transactions of the ASABE, 54, 2067-2078, 2011.

Shukla, S., Shrestha, N. K., and Goswami, D.: Evapotranspiration And Crop Coefficients for Seepage-Irrigated Watermelon with Plastic Mulch In a Sub-Tropical Region, Transactions Of the Asabe, 57, 1017-1028, 2014a.

Shukla, S., Shrestha, N. K., Jaber, F. H., Srivastava, S., Obreza, T. A., and Boman, B. J.: Evapotranspiration and crop coefficient for watermelon grown under plastic mulched conditions in sub-tropical Florida, Agricultural Water Management, 132, 1-9, 10.1016/j.agwat.2013.09.019, 2014b.

Sun, G., Noormets, A., Gavazzi, M. J., McNulty, S. G., Chen, J., Domec, J. C., King, J. S., Amatya, D. M., and Skaggs, R. W.: Energy and water balance of two contrasting loblolly pine plantations on the lower coastal plain of North Carolina, USA, Forest Ecology And Management, 259, 1299-1310, DOI 10.1016/j.foreco.2009.09.016, 2010.

Sun, G., Alstad, K., Chen, J. Q., Chen, S. P., Ford, C. R., Lin, G. H., Liu, C. F., Lu, N., McNulty, S. G., Miao, H. X., Noormets, A., Vose, J. M., Wilske, B., Zeppel, M., Zhang, Y., and Zhang, Z. Q.: A general predictive model for estimating monthly ecosystem evapotranspiration, Ecohydrology, 4, 245-255, Doi 10.1002/Eco.194, 2011a.

Sun, G., Caldwell, P., Noormets, A., McNulty, S. G., Cohen, E., Moore Myers, J., Domec, J. C., Treasure, E., Mu, Q., and Xiao, J.: Upscaling key ecosystem functions across the conterminous United States by a water - centric ecosystem model, Journal of Geophysical Research: Biogeosciences, 116, 2011b.

Sun, S., Chen, H., Ju, W., Yu, M., Hua, W., and Yin, Y.: On the attribution of the changing hydrological cycle in Poyang Lake Basin, China, Journal of Hydrology, 514, 214-225, 2014.

Sun, S., Sun, G., Caldwell, P., McNulty, S., Cohen, E., Xiao, J., and Zhang, Y.: Drought impacts on ecosystem functions of the US National Forests and Grasslands: Part II assessment results and management implications, Forest Ecology and Management, 353, 269-279, 2015a.

Sun, S., Sun, G., Caldwell, P., McNulty, S. G., Cohen, E., Xiao, J., and Zhang, Y.: Drought impacts on ecosystem functions of the US National Forests and Grasslands: Part I evaluation of a water and carbon balance model, Forest Ecology and Management, 353, 260-268, 2015b.

Tabari, H., Grismer, M. E., and Trajkovic, S.: Comparative analysis of 31 reference evapotranspiration methods under humid conditions, Irrigation Science, 31, 107-117, 2013.

Taylor, N., Mahohoma, W., Vahrmeijer, J., Gush, M., Allen, R. G., and Annandale, J. G.: Crop coefficient approaches based on fixed estimates of leaf resistance are not appropriate for estimating water use of citrus, Irrigation Science, 33, 153-166, 2015.

Tolk, J. A., and Howell, T. A.: Measured and simulated evapotranspiration of grain sorghum grown with full and limited irrigation in three high plains soils, Transactions Of the Asae, 44, 1553-1558, 2001.

Vose, J. M., Sun, G., Ford, C. R., Bredemeier, M., Otsuki, K., Wei, X., Zhang, Z., and Zhang, L.: Forest ecohydrological research in the 21st century: what are the critical needs?, Ecohydrology, 4, 146-158, 2011.

Wei, Z., Paredes, P., Liu, Y., Chi, W. W., and Pereira, L. S.: Modelling transpiration, soil evaporation and yield prediction of soybean in North China Plain, Agricultural Water Management, 147, 43-53, http://dx.doi.org/10.1016/j.agwat.2014.05.004, 2015.

Xiao, J., Ollinger, S. V., Frolking, S., Hurtt, G. C., Hollinger, D. Y., Davis, K. J., Pan, Y., Zhang, X., Deng, F., and Chen, J.: Data-driven diagnostics of terrestrial carbon dynamics over North America, Agricultural and Forest Meteorology, 197, 142-157, 2014.

Zeppel, M. J. B., Macinnis-Ng, C. M. O., Yunusa, I. A. M., Whitley, R. J., and Earnus, D.: Long term trends of stand transpiration in a remnant forest during wet and dry years, Journal Of Hydrology, 349, 200-213, DOI 10.1016/j.jhydrol.2007.11.001, 2008.

Zhang, B., Liu, Y., Xu, D., Zhao, N., Lei, B., Rosa, R. D., Paredes, P., Pa ço, T. A., and Pereira, L. S.: The dual crop coefficient approach to estimate and partitioning evapotranspiration of the winter wheat–summer maize crop sequence in North China Plain, Irrigation Science, 31, 1303-1316, 2013.

Zhang, F., Zhou, G. S., Wang, Y., Yang, F. L., and Nilsson, C.: Evapotranspiration and crop coefficient for a temperate desert steppe ecosystem using eddy covariance in Inner Mongolia, China, Hydrological Processes, 26, 379-386, 2012.

Zhang, L., Dawes, W. R., and Walker, G. R.: Response of mean annual evapotranspiration to vegetation changes at catchment scale, Water Resources Research, 37, 701-708, 2001.

Zhang, Y., Song, C., Sun, G., Band, L. E., McNulty, S., Noormets, A., Zhang, Q., and Zhang, Z.: Development of a coupled carbon and water model for estimating global gross primary productivity and evapotranspiration based on eddy flux and remote sensing data, Agricultural and Forest Meteorology, 223, 116-131, 2016.

Zhou, L., Zhou, G. S., Liu, S. H., and Sui, X. H.: Seasonal contribution and interannual variation of evapotranspiration over a reed marsh (Phragmites australis) in Northeast China from 3-year eddy covariance data, Hydrological Processes, 24, 1039-1047, 2010.

Table 1 Multiple linear regression relationships among crop coefficient and LAI, precipitation and site latitude in different seasons.

IGBP	season	*N*	R^2	*Kc*	*b*	a_1	a_2	a_3
CRO	Spring	24	0.16	0.31	0.242***	0.141*		
	Summer	24	0.21	0.57	0.331**			0.0033*
	Fall	23	0.78	0.48	0.036	0.472***		
	Winter	21	0.36	0.26	0.920***		-0.0141**	
DBF	Spring	39	0.49	0.30	0.479**		-0.0076*	0.0022***
	Summer	39	0.42	0.65	0.536***			0.0011***
	Fall	39	0.13	0.60	0.462***			0.0014*
	Winter	39	0.15	0.30	0.713***		-0.0094*	
EBF	Spring	6	-	0.66	0.663***			
	Summer	6	0.93	0.97	-2.10**		0.059**	
	Fall	4	-	0.77	0.772**			
	Winter	3	-	0.52	0.519**			
ENF	Spring	96	0.39	0.37	0.225***	0.060***		0.0017***
	Summer	99	0.59	0.49	0.211***	0.053***		0.0020***
	Fall	98	0.55	0.52	-0.040	0.066***	0.0049*	0.0025***
	Winter	92	0.21	0.44	0.293***	0.084*		0.0010*
GRA	Spring	27	0.48	0.45	0.237***			0.0052***
	Summer	27	0.23	0.86	0.572***	0.110*		
	Fall	27	0.30	0.76	0.499***	0.123**		
	Winter	27	0.26	0.41	0.256**			0.0038**
MF	Spring	30	0.67	0.31	0.099**	0.188***		0.0012***
	Summer	30	0.40	0.61	0.372***			0.0029***
	Fall	30	0.54	0.58	0.250***	0.071***		0.0018***
	Winter	30	0.13	0.33	0.961**		-0.0136*	
OS	Spring	6	-	0.23	0.230***			
	Summer	6	0.90	0.35	-5.419*		0.1005*	0.0026*
	Fall	6	0.88	0.42	-9.921*	0.051*	0.1828*	
	Winter	6	0.99	0.14	-4.919*	0.629*	0.0882*	0.0032*

Note: *N* is the number of observations used, R^2 the determination coefficient, Kc_{Ave} is the average *Kc* for seasons. *b* is the intercept of the multiple linear equation, a_1 the coefficient of LAI, a_2 the coefficient of site latitude (Absolute values), a_3 the coefficient of precipitation. IGBP is the International Geosphere-Biosphere Program land cover classification system: cropland (CRO), deciduous broad leaf forest (DBF), evergreen broad leaf forest (EBF), evergreen needle leaf forest (ENF), grassland (GRA), mixed forest (MF), and open shrubland (OS). ***, **, * stand for $p<0.001$,

$p<0.01$, $p<0.1$. Spring is the month of February, March and April; Summer is the month of May, June and July; Fall is August, September and October; Winter is November, December and January.

Figure captions

Fig. 1 Location of eddy flux sites from which climate and evapotranspiration data are collected.

Fig. 2 The variation of *Kc* for the different IGBP_code. The error ~~bras~~ are stand errors among different sites.

Fig.3 Average *Kc* at spring, summer, fall and winter in different vegetation types. The error ~~bras~~ are stand errors among different sites. Spring is the month of February, March and April; Summer is the month of May, June and July; Fall is August, September and October; Winter is November, December and January.

Fig. 4 Annual total precipitation (P), AET and PET in different vegetation types The error ~~bras~~ are ~~stand~~ errors among different sites.

Fig. 5 Variation of annual *Kc* at different latitude (Lat). (a) stand for cropland (CRO), deciduous broad leaf forest (DBF), evergreen broad leaf forest (EBF), and (b) evergreen needle leaf forest (ENF), grassland (GRA), mixed forest (MF), and open shrubland (OS). The absolute values of the latitude were used in EBF in the southern hemisphere sites and all the determination coefficient (R^2) listed in the figure were significant (p<0.05).

Fig. 6 Relationships between the average monthly *Kc* and the total monthly precipitation (P, mm) for different vegetation surfaces. (a)~(g) represent for cropland (CRO), deciduous broad leaf forest (DBF), evergreen broad leaf forest (EBF), evergreen needle leaf forest (ENF), grassland (GRA), mixed forest (MF), and open shrubland (OS). All the determination coefficient (R^2) listed in the figure were significant (p<0.001)

Fig. 7 Relationships between the average monthly *Kc* and leaf area index for different vegetation surfaces. (a)~(g) stand for cropland (CRO), deciduous broad leaf forest (DBF), evergreen broad leaf forest (EBF), evergreen needle leaf forest (ENF), grassland (GRA), mixed forest (MF), and

open shrubland (OS). All the determination coefficient (R^2) listed in the figure were significant (p<0.001)

Fig. 8 Relationships between the simulated ET using *Kc* from Table 1 (SET) and the measured ET (AET) for different vegetation surfaces. (a)~(f) stand for cropland (CRO), deciduous broad leaf forest (DBF), evergreen broad leaf forest (EBF), evergreen needle leaf forest (ENF), grassland (GRA), mixed forest (MF), and open shrubland(OS). All the determination coefficient (R^2) listed in the figure were significant (p<0.001).

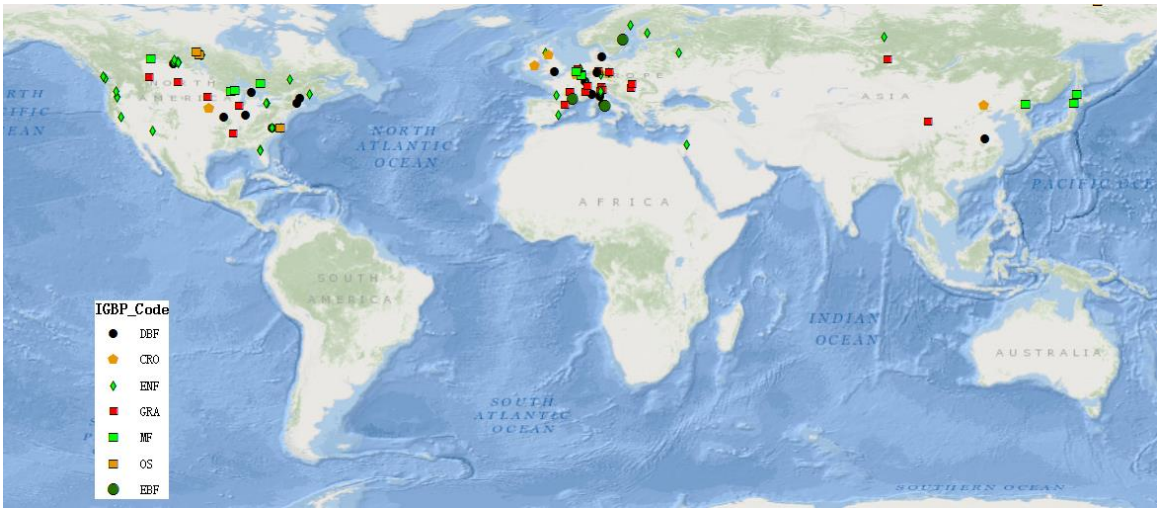

Fig. 1 Location of eddy flux sites from which climate and evapotranspiration data are collected.

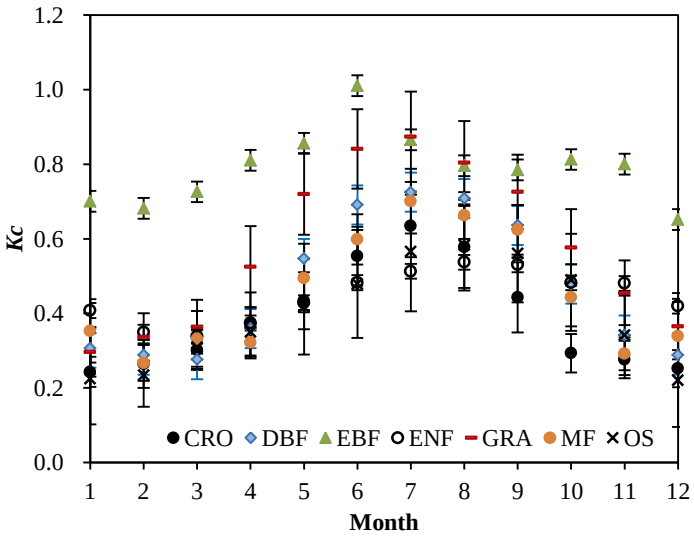

520

Fig. 2 The variation of *Kc* for the different IGBP_code. The error bras are stand errors among different sites.

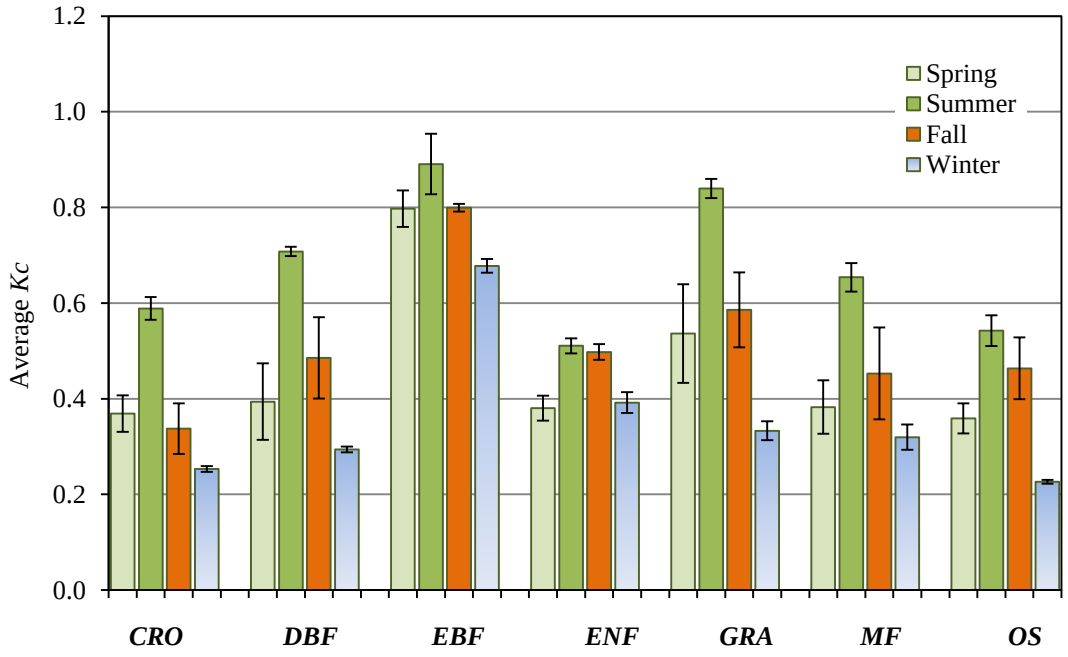

Fig.3 Average *Kc* at spring, summer, fall and winter in different vegetation types. The error bras are stand errors among different sites. Spring is the month of February, March and April; Summer is the month of May, June and July; Fall is August, September and October; Winter is November, December and January.

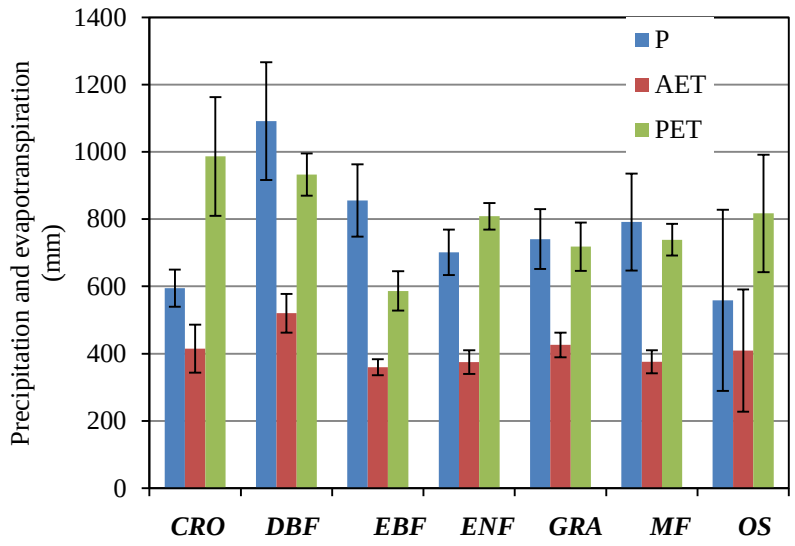

Fig.4 Annual total precipitation (P), AET and PET in different vegetation types. The error bras are stand errors among different sites.

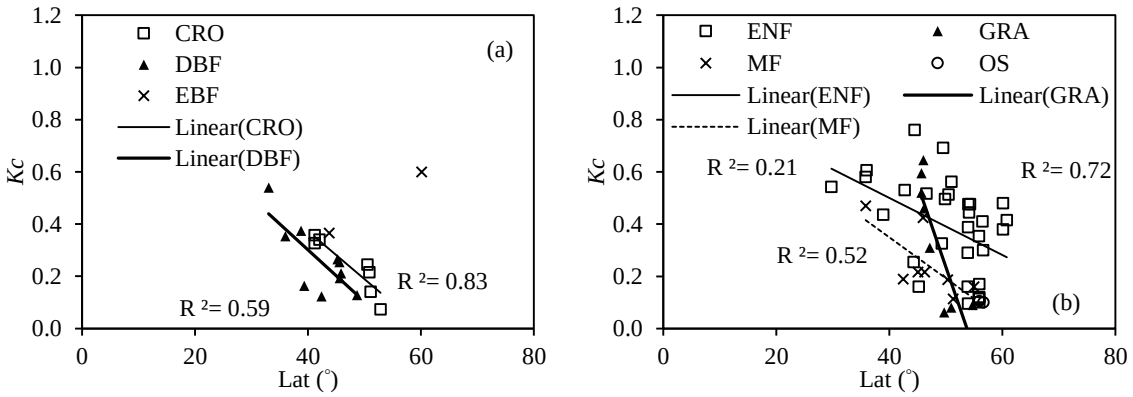

Fig. 5 Variation of annual *Kc* at different latitude (Lat). (a) stand for cropland (CRO), deciduous broad leaf forest (DBF), evergreen broad leaf forest (EBF), and (b) evergreen needle leaf forest (ENF), grassland (GRA), mixed forest (MF), and open shrubland (OS). The absolute values of the latitude were used in EBF in the southern hemisphere sites and all the determination coefficient (R^2) listed in the figure were significant (p<0.05).

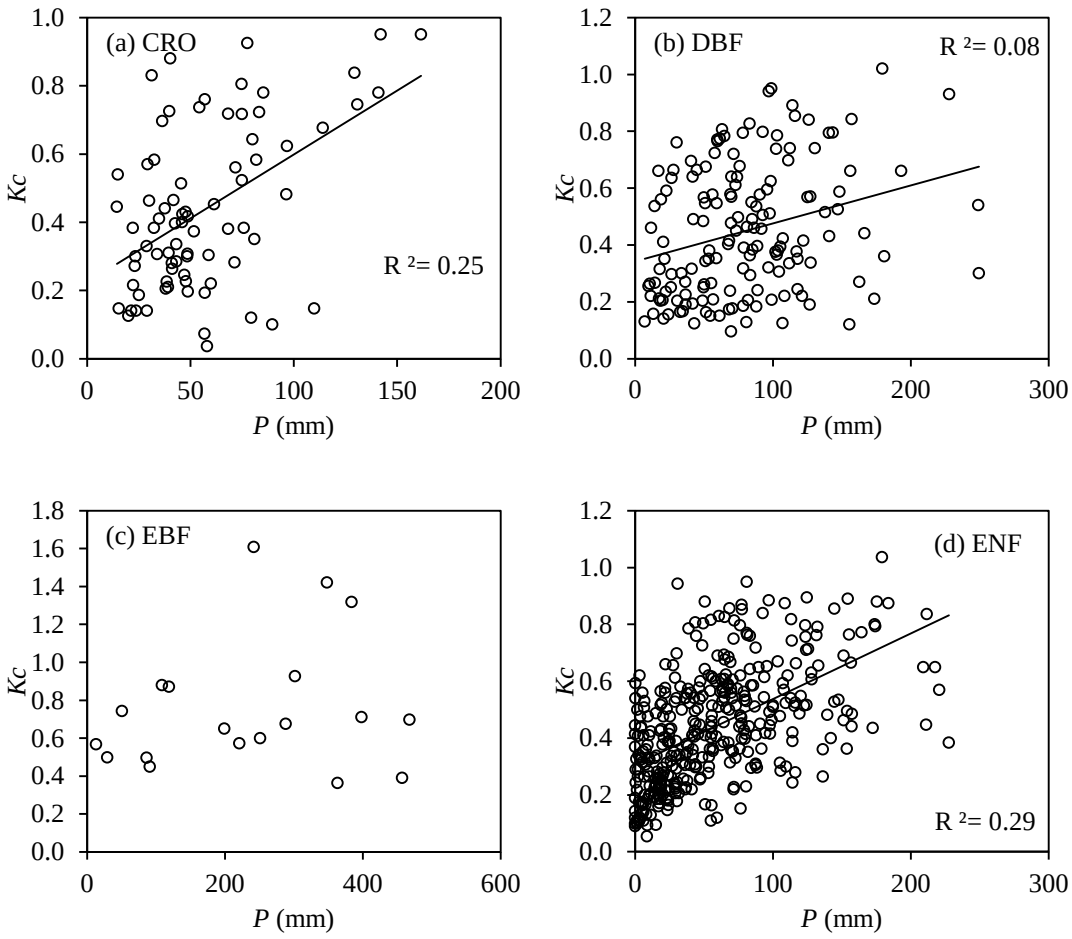
(a) CRO
R ²= 0.25
(b) DBF
R ²= 0.08
(c) EBF
(d) ENF
R ²= 0.29
Kc
P (mm)

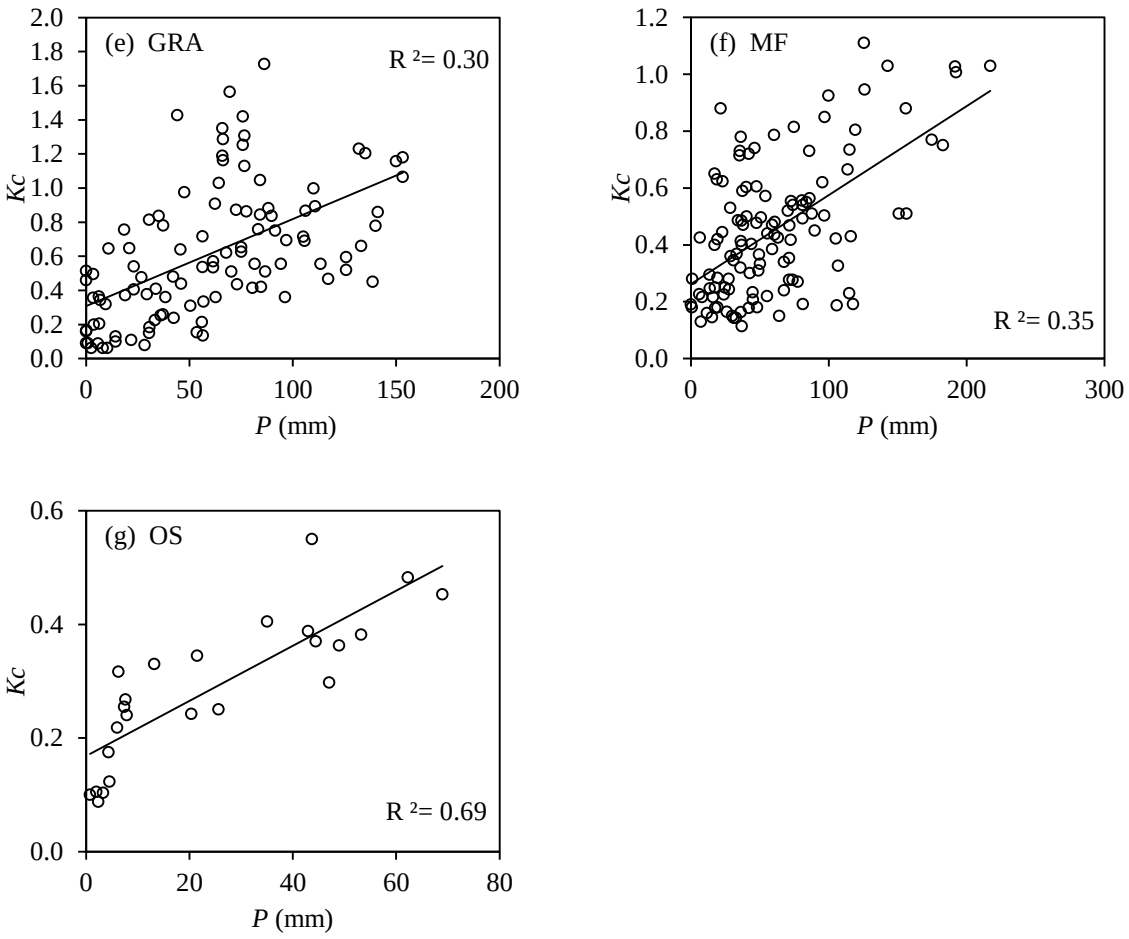

Fig. 6 Relationships between the average monthly *Kc* and the total monthly precipitation (P, mm) for different vegetation surfaces. (a)~(g) represent for cropland (CRO), deciduous broad leaf forest (DBF), evergreen broad leaf forest (EBF), evergreen needle leaf forest (ENF), grassland (GRA), mixed forest (MF), and open shrubland (OS). All the determination coefficient (R^2) listed in the figure were significant (p<0.001)

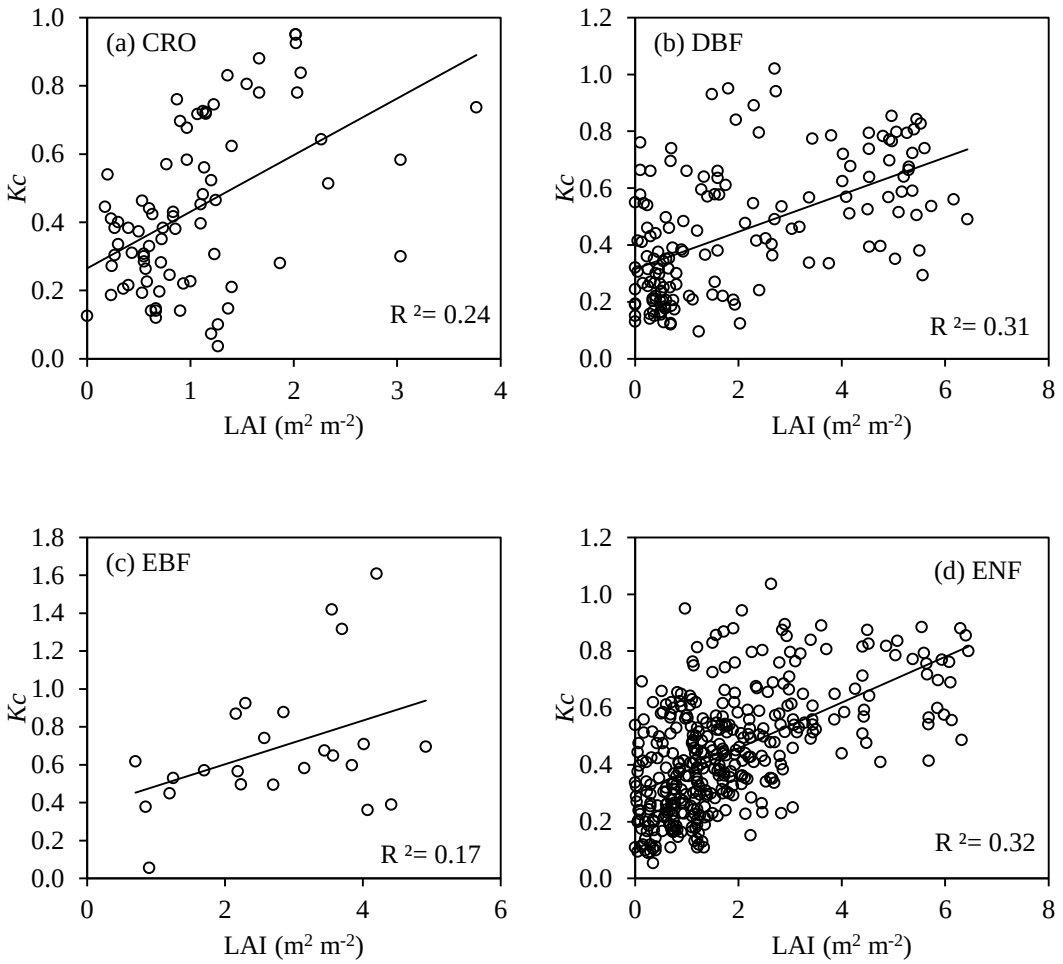

550

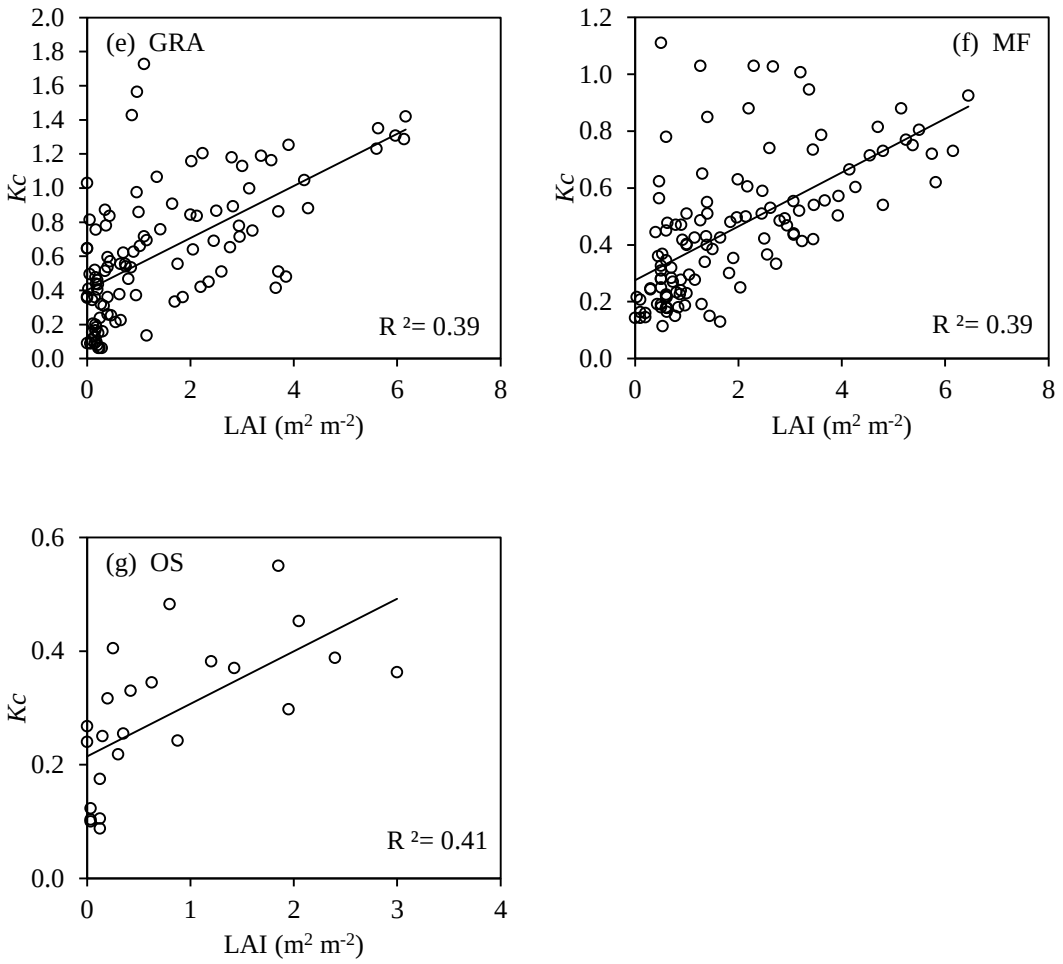

Fig. 7 Relationships between the average monthly *Kc* and leaf area index for different vegetation surfaces. (a)~(g) stand for cropland (CRO), deciduous broad leaf forest (DBF), evergreen broad leaf forest (EBF), evergreen needle leaf forest (ENF), grassland (GRA), mixed forest (MF), and open shrubland (OS). All the determination coefficient (R^2) listed in the figure were significant (p<0.05)

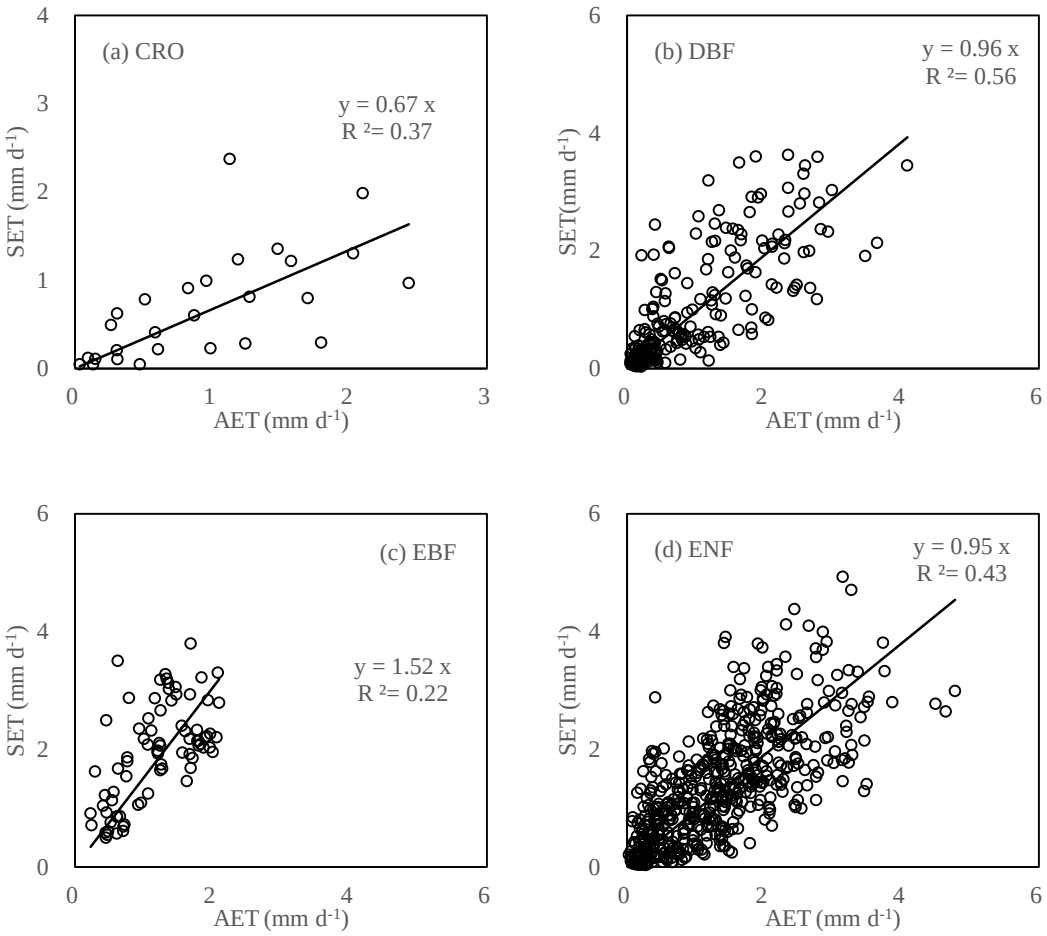
(a) CRO
y = 0.67 x
R ²= 0.37
SET (mm d-1)
AET (mm d-1)
(b) DBF
y = 0.96 x
R ²= 0.56
SET(mm d-1)
AET (mm d-1)
(c) EBF
y = 1.52 x
R ²= 0.22
SET (mm d-1)
AET (mm d-1)
(d) ENF
y = 0.95 x
R ²= 0.43
SET (mm d-1)
AET (mm d-1)

560

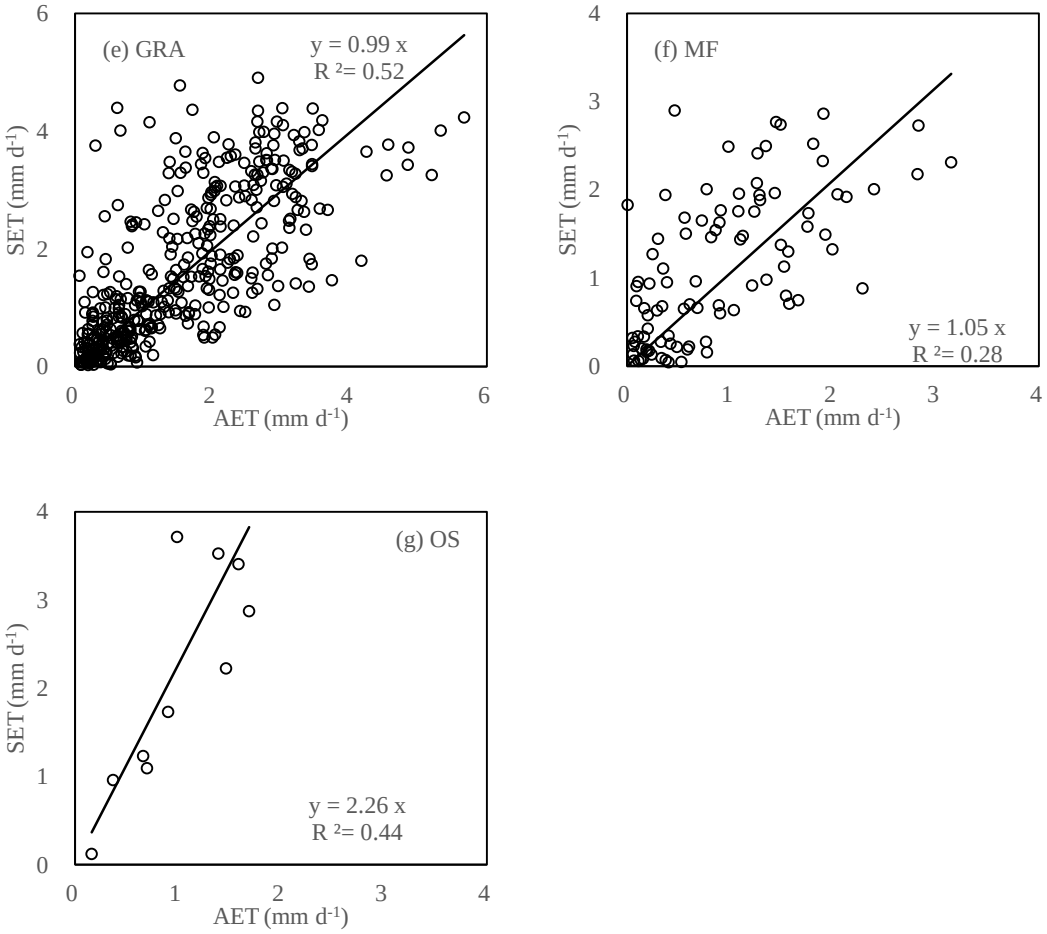

Fig. 8 Relationships between the simulated ET using *Kc* from Table 1 (SET) and the measured ET (AET) for different vegetation surfaces. (a)~(f) stand for cropland (CRO), deciduous broad leaf forest (DBF), evergreen broad leaf forest (EBF), evergreen needle leaf forest (ENF), grassland (GRA), mixed forest (MF), and open shrubland(OS). All the determination coefficient (R^2) listed in the figure were significant (p<0.001).